



Research Article

Determination of surface temperature in water bodies with the use of multiband landsat satellite images: Case study of Seyfe Lake

Cansu YURTERİ^{1,2*}, Türker KURTTAŞ³

¹Turkey Ministry of Interior, Disaster and Emergency Management Presidency, Ankara, 06800, Türkiye

²Institute of Science, Hacettepe University, Beytepe, Ankara, 06800, Türkiye

³Department of Geological (Hydrogeological) Engineering, Hacettepe University, Ankara, 06800, Türkiye

ARTICLE INFO

Article history

Received: 17 October 2021

Accepted: 27 February 2022

Keywords:

Lake Surface Temperature;
Landsat; MNDWI; Seyfe Lake;
Thermal Infrared Band

ABSTRACT

Lake Seyfe is a shallow lake 30 km east of the city center of Kırşehir with an average surface area of 34 km² and located 1110 m above sea level. Due to various interventions (via drainage and/or irrigation channels, groundwater withdrawal with wells, agricultural activities, domestic wastes, etc.) in Seyfe Lake and its surroundings from 1960s to the present, natural functions of the lake have been deteriorated. As a result of the aforementioned actions and changes such as water elevation, shrinking lake surface area, decrease in volume and changes in surface temperature were observed in the lake. In this paper, the seasonal changes in the surface temperature distribution of Seyfe Lake were analyzed with the Geographical Information Systems (GIS) using multi-band Landsat satellite images from various years. In September 1990, the lake surface temperature varied between 10.94-24.14 °C while it varied between 12.36-26.67 °C in May 1990. In May 2020, the temperatures varied between 16.31-34.06 °C, and in September 2020, it varied between 25.67-29.67 °C. When the lake surface temperature distribution was analyzed; it was determined that lower temperatures were observed in the northern parts, which are usually the deepest parts of the lake, while the temperature increased towards the central and coastal parts of the lake. However, it was seen that lake surface temperature has been affected by both climatic conditions and anthropogenic activities from the past to the present.

Cite this article as: Yurteri C, Kurttaş T. Determination of surface temperature in water bodies with the use of multiband landsat satellite images: Case study of Seyfe Lake. Sigma J Eng Nat Sci 2023;41(6):1144–1156.

INTRODUCTION

With the effect of climatic changes and global warming processes, changes in land surface temperature are observed. With these processes, rapid population growth,

reduction of green areas and increasing construction has started to threaten the natural ecological system, climate, individual and industrial efficiency. As it is known, the use of fossil fuels, industrialization and the widespread use of

*Corresponding author.

*E-mail address: cyrterti@hacettepe.edu.tr, cansu.yurteri@afad.gov.tr

This paper was recommended for publication in revised form by Regional Editor Amin Shahsavari



industrial agriculture cause an increase in the temperature on the land surface. From all these processes, the water bodies on earth (lakes, inland seas, oceans, rivers, etc.) are also affected. Lakes are sensitive water bodies and are very open systems to global climate changes and eutrophication processes. Lake water surface temperature is an important variable used to examine the functioning of the lake ecosystem and the reaction of the lake environment to climatic changes [1]. Water Surface Temperature (WST) is a result of energy balance on the water surface and heat transfer mechanisms within the water body [2]. It is also seen that the temperature change in the lake surface water affects the chemical and physical properties of the lake and the speed of biochemical activities in the lake environment [3]. Land Surface Temperature (LST) is an important indicator that controls the energy balance between the atmosphere and the earth and is identified as the radiative temperature of the earth [4]. Today, remote sensing studies carried out using thermal bands to determine the land surface temperature and the surface temperature of water bodies have become quite widespread. It has been observed that there are many studies to determine the temperature in both land areas and water bodies using remote sensed images in thermal infrared band [5-10]. The fact that thermal remote sensing data is both costless and the accuracy of the remote sensed images for large areas in different time periods is high and most importantly, easy to access provides significant convenience in the studies. With these images, it has become possible to determine the surface temperature distribution in land and sea areas. There are many methods in the literature for calculating the land surface temperature using thermal bands. In these studies, it is seen that the surface temperature distribution is determined by the researchers by developing various algorithms (temperature/emissivity separation method, single channel method, single window algorithm, split window method, land surface temperature algorithm, etc.) [11-16]. The data produced are widely used in studies carried out in disciplines such as ocean and marine sciences, meteorology, hydrogeology, hydrology, environmental geology, agriculture and forestry (plant, product pattern change, land use), spatial planning, etc.

When the studies carried out in the lake area and its surroundings in the past were examined, it was determined that a limited number of remote sensing researches were carried out in Seyfe Lake and its basin [17,18]. The researchers evaluated the change of the lake surface area for different years with spectral water index (NDVI), unsupervised classification and visual interpretation methods. There is no study in the literature to determine the seasonal change of Seyfe Lake surface temperature distribution using thermal bands using remotely sensed data. And also Seyfe Lake is one of the most important wetlands of Turkey. Wetlands, formed by natural processes, with the numerous plant and animal species they host, are important reservoirs. They are also fragile ecosystems in which the effects of climate change and anthropogenic activities are

observed dynamically [19]. Seyfe Lake is located in a closed basin and the lake area and its surroundings are a Ramsar site and have the status of "Natural Site First Degree" and "Protected Natural Area". Despite having these protection statuses, due to the anthropogenic activities (uncontrolled groundwater extraction, drainage and irrigation channels, agricultural activities, discharge of domestic and industrial waste) since the 1960s, natural functioning of the Seyfe Lake was disturbed, and now it is struggling against drying up and even disappearing. According to the old and recent satellite imagery of Seyfe Lake area and the literature, the persisting shrinkage of lake area and increasing of the water surface temperature over the years in the lake area.

Seyfe Lake is located Seyfe Closed Basin. Lakes, play an active role in the hydrological cycle and an integral part of wetland environments, are important reservoirs. They have positively impacted on surface water and groundwater supplies. The role of lakes in the hydrological cycle is intimately related to water quality, temperature, volume of stored water, groundwater recharge, ecosystem maintenance, and shoreline of the lake area. For these reasons, lakes have significant benefits (economic, social, and environmental) for the communities.

In the present research, the main objectives of this study are; (i) to determine the temporal and spatial variations in seasonal temperature of the lake surface area from Landsat imagery by using remote sensing techniques and (ii) to evaluate the effects of climate and anthropogenic factors on lake surface temperature.

According to that approaches, the seasonal (in May and September) distribution of the surface temperature of Seyfe Lake from 1990 to 2020 was determined in the GIS environment. Landsat multi-band satellite images (Landsat 8 OLI/TIRS, Landsat 5 TM) were used as remote sensing data. In this context, firstly, the area covered by the lake surface from 1990 to 2020 was determined by the Modified Normalized Difference Water Index method (MNDWI) proposed by Xu [20]. Then, the lake surface temperature was determined using the thermal bands of Landsat 5 and Landsat 8 satellites. Seasonal lake surface temperature distribution was created in the Geographic Information Systems (GIS) by masking the lake surface areas and the LST maps obtained. In addition, the relationship between the density of vegetation in the lake area and its surroundings and the land surface temperature was interpreted. The steps of the method used are presented in the Material and Method section.

MATERIALS AND METHODS

Research Area Profile

The research area covers Seyfe Lake and its surroundings, located at an altitude of 1110 m from the sea, 30 km east of Kırşehir city center. Seyfe Lake, which has an average surface area of 34 km², is located between 34°22'-34° 30'

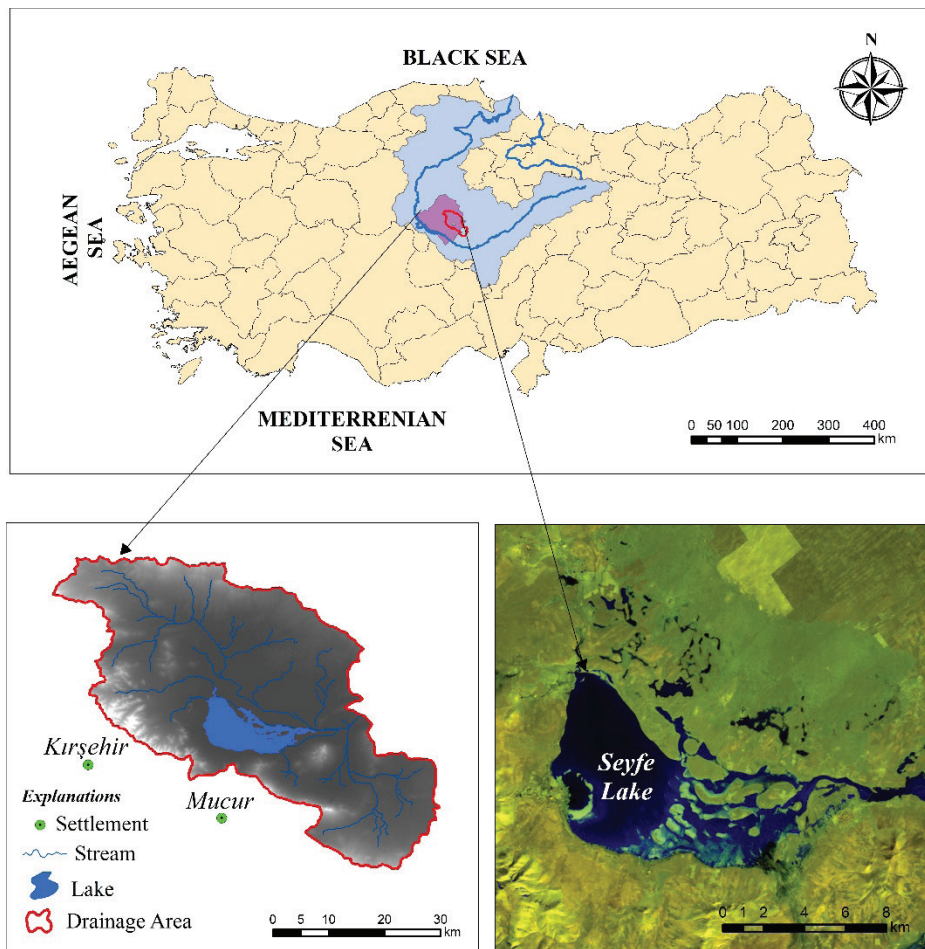


Figure 1. Location map of Seyfe Lake and its surroundings.

East longitudes and $39^{\circ} 11' - 39^{\circ} 14'$ North latitudes (Figure 1). The lake is located in Seyfe closed basin and there is no outflow from the lake. The lake area is recharged by precipitation that fall onto the lake and /or into the basin, surface flow and feeding from aquifer units in the lake basin. The discharge of the lake takes place through evaporation and drainage channels. The lake is a shallow lake and the deepest part of the lake is determined as the north of the area with 1.95 m within the scope of bathymetric evaluations.

Seyfe Lake and its surroundings from the 1960s to the present day due to various interventions (drainage or irrigation channels, wells and groundwater attraction, agricultural activities, discharge of domestic wastes, etc.) the natural functioning of the lake has deteriorated. In addition, it is thought that the change in land use over the years in Seyfe Basin, where the lake area is located, is very effective in changing the surface temperature distribution.

Satellite Data

Within the scope of the study, multi-band Landsat 5 TM and Landsat 8 OLI/TIRS multi-band satellite images were used as remote sensing data. Satellite images were downloaded from the Earth Explorer portal of the United States

Geological Survey Centre (USGS) [21]. Landsat 5 TM and Landsat 8 OLI/TIRS satellites are widely used to determine the temperature distribution using thermal bands. The Landsat 8 satellite, which uses remote sensing images within the scope of the study, has an orbit synchronized with the sun at an altitude of 705 km sent to space in February 2013 and rotates around the world in 98.8 minutes. The satellite has 2 detection sensors, the Operational Land Imager (OLI) and the Thermal Infrared Sensor (TIRS). In NDVI and MNDWI analyses, the Landsat 8 satellite had a spatial resolution of 30 meters in the OLI sensor, 4. (Red), 5. (Near Infrared), 3. (Green) and 6. (Short Wave Infrared) multi-spectral bands were used. The path and row of the Landsat images are 176 and 033, respectively. In determining the temperature distribution, the thermal band number 10 with a spatial resolution of 100 meters in the TIRS sensor was used. Another data source, the Landsat 5 TM satellite, has 2 (Green), 5 (Short Wave Infrared), 3 (Red) and 4 (Near Infrared) multispectral bands with a resolution of 30 meters. In determining the LST, the thermal band number 6 with a spatial resolution of 120 meters was used (Table 1 and Table 2). All images used were selected to represent different seasonal periods, with cloud-free.

Table 1. Characteristics of the bands used as remote sensing data in the study

Landsat 8 OLI/TIRS		Landsat 5 TM	
Bands	Wavelength (µm)	Bands	Wavelength (µm)
Band 2-Blue	0.45-0.51	Band 2-Green	0.52 - 0.60
Band 3-Green	0.53-0.59	Band 3- Red	0.63 - 0.69
Band 4- Red	0.64-0.67	Band 4-Near Infrared	0.76 - 0.90
Band 5-Near Infrared	0.85-0.88	Band 5- Shortwave Infrared	1.55 - 1.75
Band 6-SWIR-1	1.57-1.65	Band 6-Thermal Infrared	10.40 - 12.50
Band 10-TIRS-1	10.6-11.19		

Table 2. Satellite images and features used for thermal remote sensing studies in the study area

Acquisition Date	Path/Row	Satellite/Sensor	Thermal Band	Radiometric Resolution (bits)	Spatial Resolution (m)	Temporal Resolution (day)
08.05.1990	176/033	Landsat 5 TM	6	8	30	16
21.09.1990	176/033	Landsat 5 TM	6	8	30	16
14.05.1995	176/033	Landsat 5 TM	6	8	30	16
03.09.1995	176/033	Landsat 5 TM	6	8	30	16
11.05.2000	176/033	Landsat 5 TM	6	8	30	16
16.09.2000	176/033	Landsat 5 TM	6	8	30	16
25.05.2005	176/033	Landsat 5 TM	6	8	30	16
14.09.2005	176/033	Landsat 5 TM	6	8	30	16
07.05.2010	176/033	Landsat 5 TM	6	8	30	16
28.09.2010	176/033	Landsat 5 TM	6	8	30	16
05.05.2015	176/033	Landsat 8 TIRS	10	16	100	16
26.09.2015	176/033	Landsat 8 TIRS	10	16	100	16
18.05.2020	176/033	Landsat 8 TIRS	10	16	100	16
07.09.2020	176/033	Landsat 8 TIRS	10	16	100	16

Methodology

In this research, the surface temperature distribution of Seyfe Lake was determined in several steps in May and September of 1990 and 2020 using Landsat 5 TM and Landsat 8 OLI/TIRS multi-band satellite images. Basically, the temperature distribution was determined in the GIS environment on the basin scale with ArcMap 10.4.1 software using the Land Surface Temperature Algorithm, and the lake area was masked. The processes related to the method followed are given in Figure 2 as a flow chart.

Derivation of spectral radiance values from pixel values

The first step in determining the temperature distribution for the study area is to convert the pixel values into radiance values. The pixel value known as Digital Number (DN) includes the electromagnetic energy value reflected from any region [22]. These raw values need to be processed by turning them into physically meaningful data. For this reason, it is necessary to derive the spectral radiance

values by using radiometric scaling factors of the pixel values of thermal images. The following equation proposed by Chander et al., [22] is used for the conversion to radiance value using the pixel values of the thermal infrared band, which is the 6th band of Landsat 5 TM images (Equation 1).

$$L\lambda = \frac{L_{max}-L_{min}}{Q_{catmax}-Q_{catmin}} \times (Q_{cal} - Q_{catmin}) + L_{min} \quad (1)$$

Lmin and Lmax in this equation refers to: The minimum and maximum radiance values scaled according to Qcalmin and Qcalmax, Qcalmax: Calibrated maximum brightness value, Qcalmin: Calibrated minimum brightness value, Qcal: Quantized and calibrated pixel value of the satellite image and Lλ: Spectral Radiance Value W/(m²* sr * µm).

The Lmax, Lmin, Qcalmax and Qcalmin parameters used in the calculations are taken from the MTL coded metadata file of the satellite data. The values of the parameters used in the equation for the Landsat 5 satellite are given in Table 3.

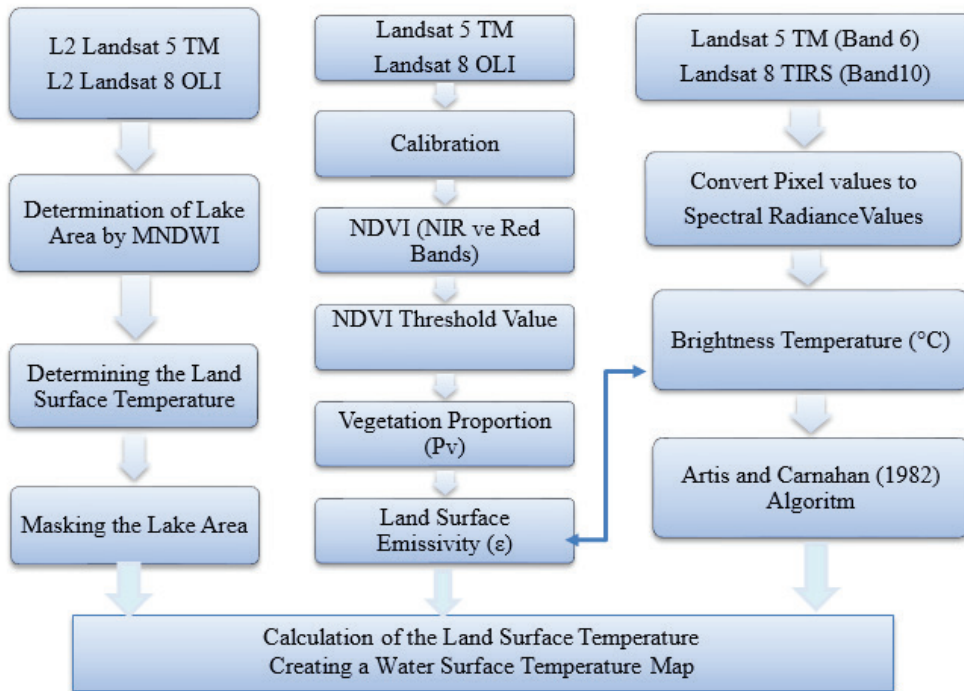


Figure 2. Flow chart for determining the temperature change of the lake surface area with satellite images.

Table 3. Parameter values used in the conversion calculations for the thermal band of the Landsat 5 satellite

L_{max}	L_{min}	Satellite/Sensor	Band	$Qcal_{min}$	$Qcal_{max}$
15.303	1.238	Landsat 5 TM	6	1	255

Landsat 8 TIRS images have two thermal infrared bands (10th and 11th bands). However, for the purpose of this study, only the pixel values of the band number 10 are used. Accordingly, the following equation proposed by USGS, [23] is used for the conversion of the band 10 to radiance values using the pixel values (Equation 2).

$$L\lambda = ML * Qcal + AL \tag{2}$$

In this equation, $L\lambda$ refers to the Spectral Radiance value ($W/(m^2 * sr * \mu m)$), $Qcal$ refers to the calibrated standard pixel value of the satellite image, AL refers to the Radiance additional rescaling factor for the processed band, and ML refers to the Radiance multiplicative rescaling factor for the processed band.

AL and ML parameters are taken from the metadata file of the satellite with MTL extension (Table 4). All equations

Table 4. Values of the parameters used in the conversion calculations for the thermal band of the Landsat 8 satellite

ML	Satellite/Sensor	Band	AL
0.0003342	Landsat 8 TIRS	10	0.10000

used were obtained from the user manuals of Landsat 5 TM and Landsat 8 OLI/TIRS satellites.

Derivation of brightness temperatures from spectral radiance values

As the second step in determining the lake surface temperature distribution, the radiance values of Landsat 5 TM and Landsat 8 TIRS satellites in thermal band sensors should be converted to brightness temperature values. In this regard, the following equation proposed by Chander et al., [22] is used. The thermal variability coefficients in the equation are obtained from the MTL coded metadata file.

$$TB = \frac{K_2}{\ln\left(\frac{K_1}{L\lambda}\right)+1} - 273.15 \tag{3}$$

In this equation, $L\lambda$ refers to the spectral radiance value, K_1 and K_2 refers to the first and second thermal conversion constants of the satellites, and TB refers to the brightness temperature value ($^{\circ}C$) (Equation 3). And also brightness temperature value is converted to the widely used unit Celsius, by adding absolute zero. The K_1 and K_2 conversion constants used for Landsat 5 and Landsat 8 are given in Table 5.

Table 5. Thermal conversion constant values of Landsat satellites and characteristics of the used bands

Satellite/Sensor	K1	K2	Band	Wavelength (μm)
Landsat 5 TM	607.76	1260.56	B6	11.45
Landsat 8 TIRS	774.89	1321.08	B10	10.89

Although the results obtained according to this equation are temperature data, it is stated that it does not represent the actual surface temperature [24]. For this reason, land surface emissivity (ϵ) correction was needed and the real land surface temperature was reached by making emissivity corrections. The corrected land surface emissivity calculation was calculated by deriving from the NDVI index and Vegetation Proportion (Pv) parameters. For this reason, NDVI and Vegetation Proportion components were calculated before the emissivity calculation was made.

Normalized difference vegetation index (NDVI)

NDVI index should be calculated in order to determine the land surface emissivity within the scope of the study. NDVI method refers to the reflection values of vegetation in nature. While plants give low reflection values in the visible red band (red) region, they give high values in the near infrared band (NIR). These bands correspond to 3rd (0.63 -0.69 μm) and 4th (0.76- 0.90 μm) bands of Landsat 5 TM satellite, and 4th (0.64-0.67 μm) and 5th (0.85-0.88 μm) bands of Landsat 8 OLI/TIRS satellite. The ratio of the difference between these bands and their sum is equal to the NDVI index (Equation 4).

$$NDVI = \frac{NIR-Red}{NIR+Red} \quad (4)$$

In this equation NIR and Red refer to the reflectance of the Near Infrared and the Red bands, respectively. NDVI index values vary between -1 and 1 [25]. It is stated that where this value is close to 1, green and healthy vegetation is high, and places between -1 and 0 point to areas with weak and no vegetation [25]. The reflection value of the NDVI value was used in the analyses made for the study area. The NDVI value obtained with the help of Equation 4 was used in the calculations of vegetation proportion and land surface emissivity.

Determination of vegetation proportion (Pv) from NDVI index

Another parameter required to determine the land surface emissivity is the vegetation rate. The vegetation ratio corresponds to the percentage of green vegetation in a pixel [26]. The Vegetation Proportion for the study area was calculated with the equation proposed by Carlson and Ripley [26] using the minimum and maximum values of the NDVI index calculated for the study area (Equation 5).

$$Pv = \left(\frac{NDVI - NDVI_{min}}{NDVI_{mak} - NDVI_{min}} \right)^2 \quad (5)$$

The Vegetation Proportion calculated for the study area was calculated with the help of Equation 5 and used in land surface emissivity calculations.

Calculation of land surface emissivity (ϵ)

One of the parameters required to calculate the land surface temperature is the land surface emissivity. Land surface emissivity is a measure of the radiation and absorption capacities of surfaces [27]. There are many equations in the literature for the calculation of surface emissivity. Emissivity value within the scope of this study has been calculated by using land vegetation (NDVI) values. In the NDVI analysis made for the study area, the equation proposed by Wang et al., [11] and the emissivity calculation were made because the field represented a pattern of mixed vegetation and bare soils (Equation 6).

$$\epsilon = 0.004 * Pv + 0.986 \quad (6)$$

The land surface emissivity was calculated using the NDVI index and Vegetation Proportion (Equation 4 and Equation 5) parameters for the study area.

Calculation of land surface temperature

After determining the corrected land surface emissivity for the study area, the real surface temperature was calculated. This value is calculated with the help of the land surface temperature algorithm proposed by Artis and Carnahan, [16] which includes land surface emissivity, thermal band and black body radiation parameters (Equation 7).

$$LST = \frac{Tb}{1 + \left(\frac{Tb}{\frac{h \times c}{s}} \times \lambda \right) \times \ln \epsilon} = \frac{Tb}{1 + \left(\frac{Tb}{C_2} \times \lambda \right) \times \ln \epsilon} \quad (7)$$

In this equation, LST indicates Land surface temperature (Kelvin), Tb: Sensor brightness temperature value (°C), ϵ : Land surface emissivity, C_2 : $(h \times c)/s = 1.44 \times 10^{-23}$ mK, s: Stefan Boltzmann Constant (1.3806×10^{-23} J/K), λ : Wavelength to thermal band (10.89 μm for Landsat 8, 11.45 μm for Landsat 5), c: Velocity of light (2.99×10^8 m/s) and h: Planck's Constant (6.63×10^{-34} J.s) values.

Delineating of lake area by using mndwi (modified normalized difference water index)

After determining the land surface temperature for the basin, the lake surface area was delineating by MNDWI method and distributed the LST by masking the lake area.

Today, with the developing satellite technology, the surface area boundaries of water bodies in various parts

of Turkey and the world can be determined by spectral water index equations. Spectral water indices (MNDWI, Normalized Difference Water Index (NDWI)) are widely used in lakes and wetlands, especially in the delineation of water bodies and land covers. These index equations are based on the ratio of the difference between the wavelengths of the selected bands and their sums. Within this framework, the change in the Seyfe Lake surface area was investigated by the Modified Normalized Difference Water Index (MNDWI) method proposed by Xu, [20] by using Landsat multi-band satellite images (Landsat 5 TM, Landsat 8 OLI/TIRS) with path/row number 176/033 in the study area.

MNDWI method is the modified version of NDWI. In the MNDWI method uses the Middle Infrared Band (MIR) instead of the Near Infrared Band (NIR) in NDWI. Because in this method, an area covers with water is absorbed more light in the area of the MIR band than NIR region. It was determined that the MNDWI method proposed by Xu, [20] achieved more effective and accurate results in the detection of water bodies compared to the results obtained with the other spectral water indices. In MNDWI has the capability of reducing the effects of soil, land, settlements, impermeable surfaces and vegetation can be separated more clearly, areas covered with water are determined more clearly, and the shadow effect on land objects disappears Xu, [20]. Within the scope of the research, all analysis and calculations for determining where the lake area is covered with water were carried out with ArcMap 10.6.1 software in the CBS environment. In the raster data obtained by MNDWI analysis, positive values are defined as areas covered with water, and values less than 0 are defined as terrestrial areas (settlement, soil, land vegetation, etc.). MNDWI equation can be expressed as shown in the Equation 8.

$$MNDWI = \frac{Green - SWIR}{Green + SWIR} \quad (8)$$

Where Green, is the reflectance of Green band and SWIR is the reflectance of the shortwave infrared band of Landsat 8 (Landsat 5 TM bands Green and MIR, respectively). MNDWI has been calculated using Landsat imagery to estimate the area of Seyfe Lake from 1990 to 2020. MNDWI values vary between -1 and +1 in the study area (Figure 4-5). MNDWI raster data has classified into non water and water classes and a threshold value was set to zero. According to the MNDWI results of the study area; values between 0 and 1 are defined as areas covered with water, and values less than 0 was defined as terrestrial areas (settlement, soil, land vegetation, etc.).

RESULTS AND DISCUSSION

NDVI Analysis for the Study Area

NDVI values in the study area vary between -1 and +1 as expected. The NDVI index is a measure of the amount of plant chlorophyll and shows the lowest values where water surfaces are present and settlements are present. NDVI values in Seyfe Lake, which is the study area, take the lowest values in the lake area and its surroundings (values close to -1 and 0). In the southwest of the study area, it is seen that NDVI values have the highest values in the areas where vegetation (agricultural areas, intermittent bushes and natural meadows) are dense. However, while the land surface temperatures were low in areas with dense and healthy vegetation, it was determined that the land surface temperatures were higher in areas with non vegetation or weak vegetation (Figure 3).

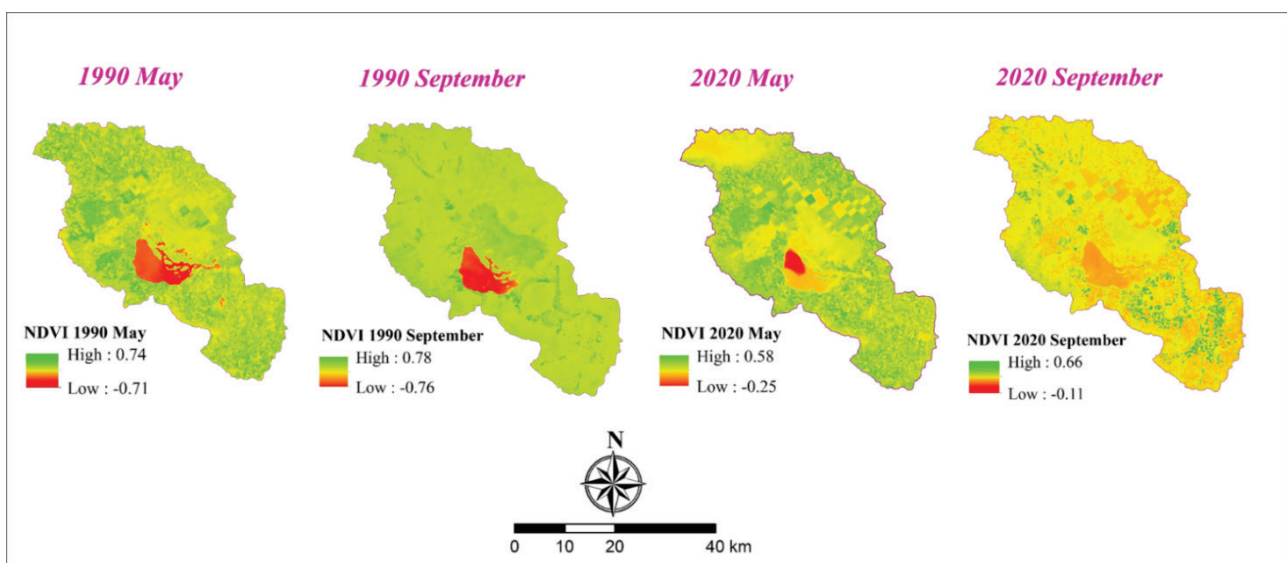


Figure 3. NDVI values in the study area

Temporal Change of Lake Surface Temperature Distribution

As a result of the studies conducted in Seyfe Lake area and basin, lake surface areas from 1990 to 2020 were determined using the Modified Normalized Difference Water Index method. Then, thermal infrared images of Landsat 5 and Landsat 8 satellites were used to derive temperature

data. In this context, firstly, the pixel values of thermal bands were converted to the top of atmospheric spectral radiance values by using scaling factors. Spectral radiance values were converted to brightness temperatures. Although the brightness temperature values here are temperature data, since it does not reflect the actual temperature values, the land surface emissivity was corrected and the actual

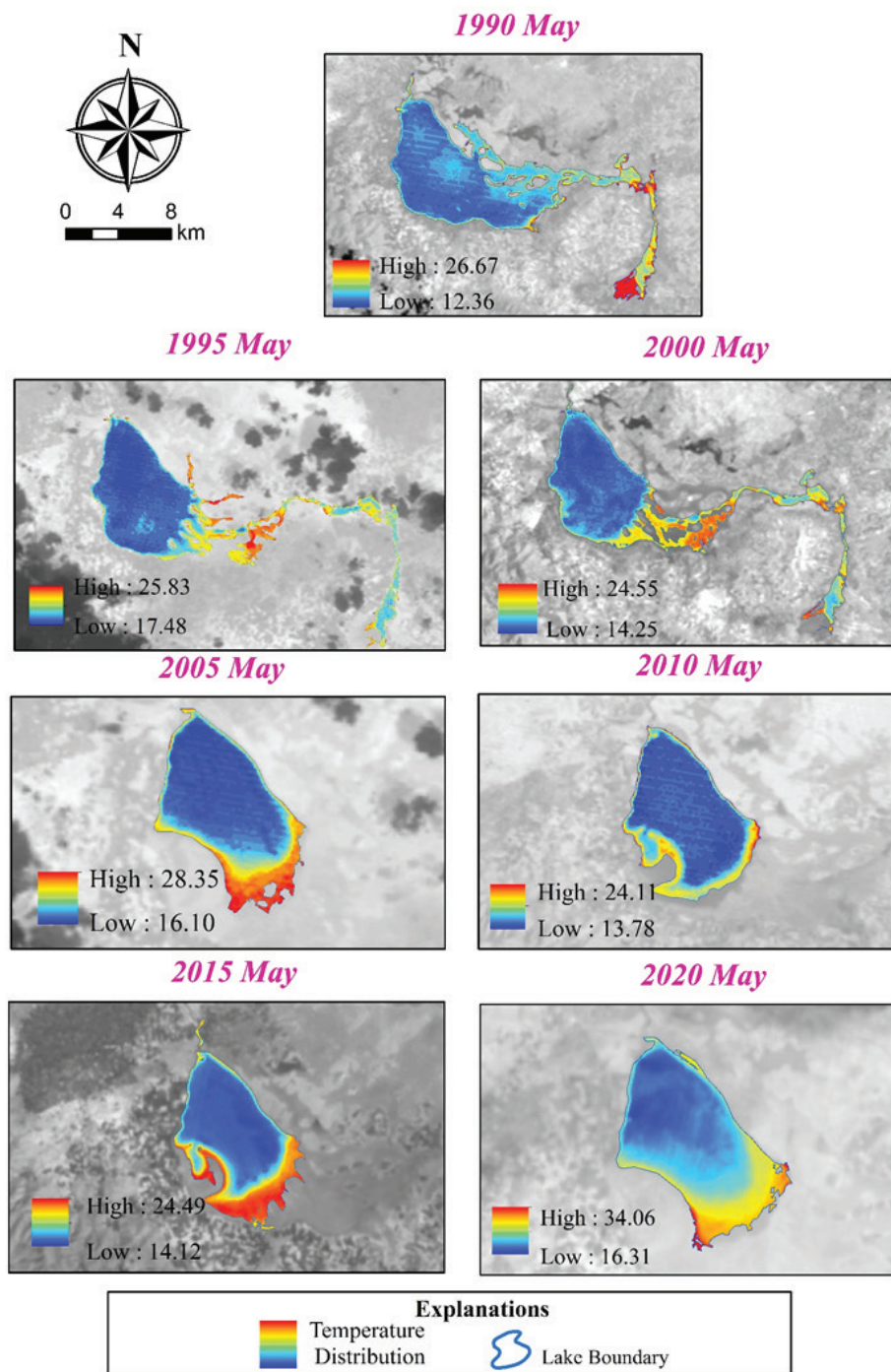


Figure 4. Seyfe Lake surface temperature distribution from 1990 to 2020 (in May) and lake surface boundaries extracted by MNDWI method.

temperature values for the study area were determined. However, in order to determine the land surface emissivity, the Vegetation Proportion (Pv) parameters derived from the NDVI and NDVI index were needed and determined with the help of the equations proposed by the researchers in the literature [25]. By calculating these values, the real land surface temperature values for the study area were reached. As a final stage, the seasonal surface temperature values calculated for the Seyfe Basin were masked for the lake areas determined by the MNDWI method and the lake

surface temperature distribution was created (Figure 4 and Figure 5).

Seasonal lake surface temperature statistics for the period between 1990 and 2020 are given in Table 6. Accordingly, while the lake surface temperature varies between 12.36-26.67 °C in May 1990, it varies between 10.94-24.14 °C in September 1990. 2020 in May, temperatures vary between 16.31-34.06 °C, while 2020 in September, temperatures vary between 25.67-29.67 °C. While the mean lake surface temperature was 15.15 °C in May 1990, it was determined

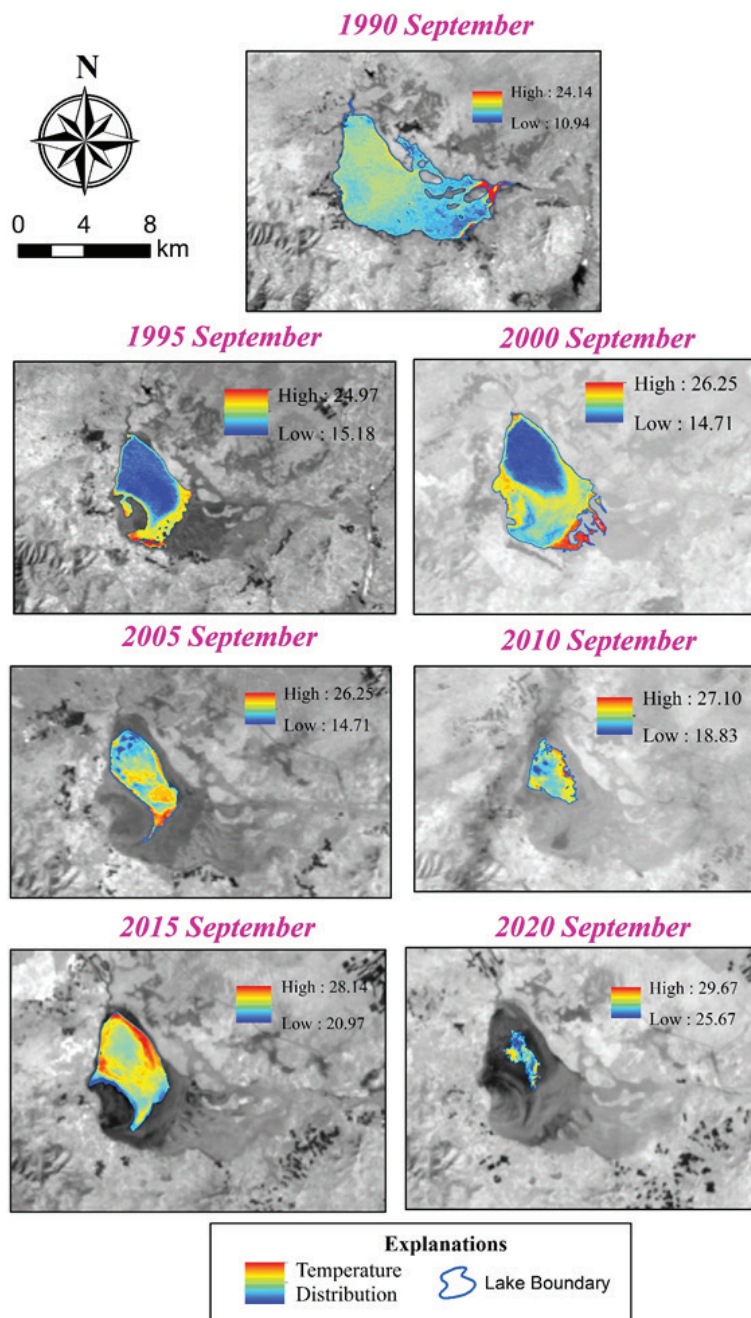


Figure 5. Seyfe Lake surface temperature distribution from 1990 to 2020 (in September) and lake surface boundaries extracted by MNDWI method.

Table 6. Seasonal temperature values of Seyfe Lake surface area

Year-Time	Maximum WST (°C)	Minimum WST (°C)	Mean WST (°C)	Monthly Mean Air Temperature (°C)	Lake Surface Area (km ²)
1990 May	26.67	12.36	15.15	13.5	82.65
1990 September	24.14	10.94	13.60	18.6	65.90
1995 May	25.83	17.48	19.75	16.2	56.56
1995 September	24.97	15.18	17.97	18.7	26.95
2000 May	24.55	14.25	17.42	14	56.67
2000 September	26.25	14.71	18.82	18.5	37.29
2005 May	28.35	16.10	19.59	15.3	22.45
2005 September	27.93	19.73	23.81	18.1	12.50
2010 May	24.11	13.78	15.70	16.3	30.58
2010 September	27.10	18.83	23.08	21.6	7.62
2015 May	24.49	14.12	17.72	16	33.88
2015 September	28.14	20.97	25.13	23	18.03
2020 May	34.06	16.31	22.17	15.9	22.05
2020 September	29.67	25.67	27.26	22.8	2.74

as 13.60 °C in September 1990. The mean lake surface temperatures in May and September 2020 are 22.17 and 27.26 °C. Changes in lake water mean temperatures were 1.55 °C in 1990 and 5.09 °C in 2020 (Table 6).

The lake surface temperatures determined for the selected time series were compared with the monthly mean air temperature data of the closest meteorological station to the study area. In this regard, monthly mean

air temperature data measured in Kırşehir Meteorology Station were examined.

Accordingly, it is seen that the mean lake surface temperature values in May and September 1990 are compatible with the monthly mean air temperature data in May and September 1990 and that the lake area reflects the seasonal temperature. As seen in Figure 6 and 7 there was a decline in the lake area from 1990 to 2005, lake surface temperature values did increase inversely. The decrease in the area values

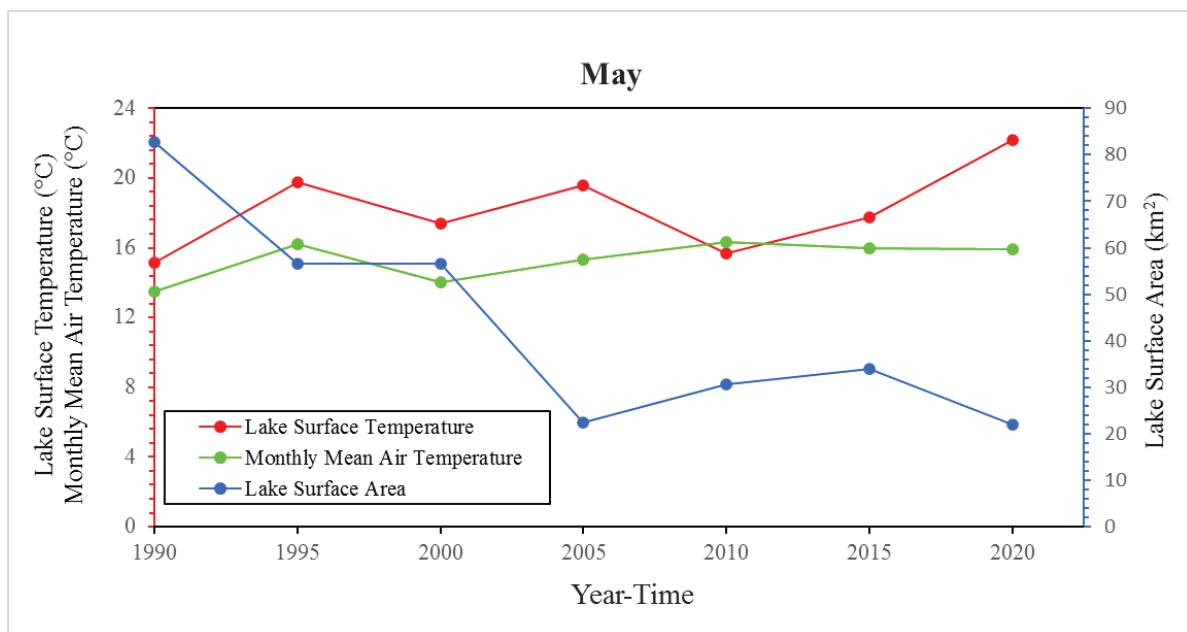


Figure 6. Relationship between Seyfe Lake surface temperature, lake surface area and monthly mean air temperature data from 1990 to 2020 (May).

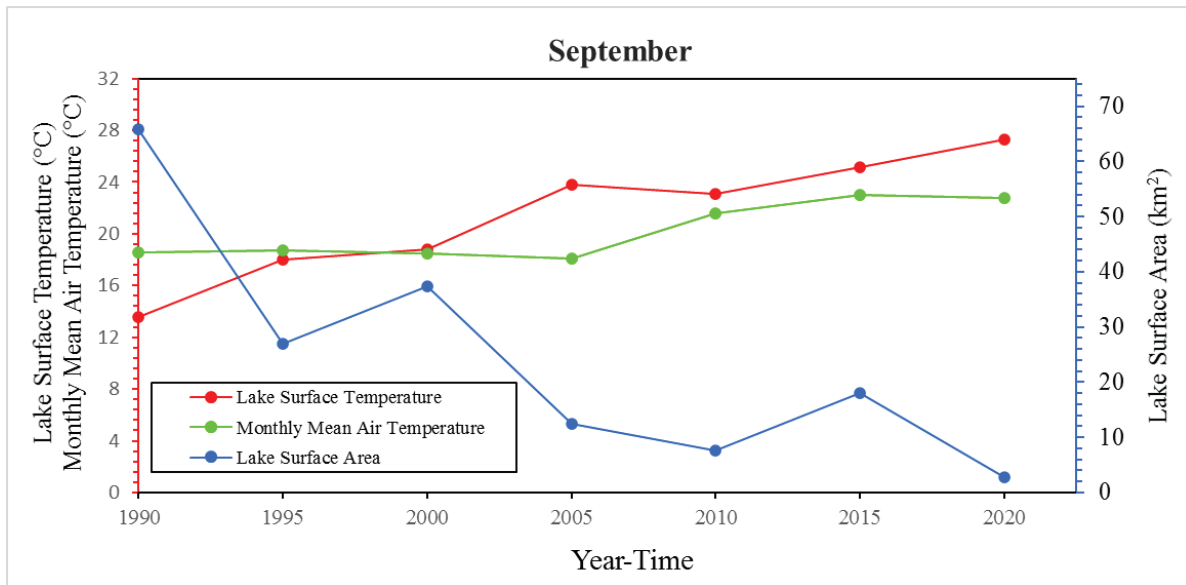


Figure 7. Relationship between Seyfe Lake surface temperature, lake surface area and monthly mean air temperature data from 1990 to 2020 (September).

from 1990 to the end of 2005 and the increase in 2005 and 2015 are inversely proportional to the change in lake temperature and mean air temperature values in the same periods. Although the decrease in the lake area between 1990 and 2005 was also inversely proportional to the increase in the temperature values, the temperature values continued to increase between 2010 and 2020 despite the lake area slightly increase during this period. The increase in lake area values between 2005 and 2010 results a decrease in the temperature values. This was interpreted as the fact that the anthropogenic effects in the lake area were very low in 1990 and the components affecting the natural balance of the lake were limited to climatic factors. By 2020, it is thought that climatic changes and anthropogenic effects in the 30-year period cause an increase in lake surface temperature (Table 6). In addition, due to the gradual decrease in the lake surface area, the deterioration of the lake water quality, the increase in the amount of evaporation in the summer months, the increase in the salt concentration in the lake waters and the terrestrial effect in the climatic conditions in the lake basin are thought to increase. Therefore, as a result of all these processes, it is observed that the lake surface temperatures are higher than the average air temperature (Figure 6 and Figure 7).

In addition, when the lake surface temperature distribution for the period between 1990 and 2020 was examined, it was determined that while lower temperatures were observed in the northern parts of the lake, which is the deepest part of the lake, the temperature increased towards the central and coastal parts of the lake. The lake is a shallow lake and the lake area and its surroundings have low slope (0-5°) topography. Therefore, seasonal changes in the lake water level and surface area are visibly noticed. For this

reason, it is thought that the surface temperatures in the coastal parts of the lake are more variable and higher than inland parts.

CONCLUSIONS

Lakes are fragile ecosystems that are easily altered by climatic and anthropogenic activities. Especially shallow lakes easily degraded by a combination of human activities and environmental factors.

In this research, the seasonal lake surface area between the years of 1990-2020 was determined using the MNDWI water index. Then, the land surface temperature distribution of the lake area was determined using the thermal infrared bands of Landsat 5 TM and Landsat 8 OLI/TIRS satellites. In this temperature distribution, lake surface temperatures were determined for May and September from 1990 to 2020 by masking the areas covered with the lake.

According to the analyzes, the mean lake surface water temperature changes were 1.55°C in 1990 and approximately 5.09°C in 2020. It was calculated that 1.42-2.53 °C changes between the minimum and maximum temperatures of lake water in May and September 1990 and 4.39-9.36 °C changes in 2020. And also seasonally mean lake surface temperature has increased between 6.92-8.57 °C from 1990 to 2020. The calculating water surface temperature estimates were highly in accordance with mean air temperature values. Generally, in September, the lake temperatures are higher than the air temperatures. And also an estimated land surface temperature is negatively correlated with NDVI values of the lake area

Since 1990, the calculated lake surface temperature values show a general rising trend, consistent with the climatic

factors and human activities. And also it was observed that there was an increase in the surface temperature of the lake due to the shrinkage in the lake area.

In this context, it is thought that climatic changes and anthropogenic factors have an effect on the change in lake surface water temperature over the years. Furthermore, calculated the land surface temperature (LST) results highlighted declining surface area and rising water temperatures are a major concern and also Seyfe Lake at risk of drying up. And also the results of the study reveal that how shallow lakes are susceptible to climate change and human caused factors.

When the lake surface temperature distribution during the period between 1990 and 2020 was examined, it was determined that while lower temperatures were observed in the northern parts of the lake, which is the deepest part of the lake, the temperature increased towards the central and coastal parts of the lake. In addition, lower temperatures were observed in places where the vegetation was dense in the lake basin, while relatively higher land surface temperatures were observed in places where the vegetation was almost nonexistent or very low.

Within the scope of the researches aimed at furthering this study, it is thought that the lake surface temperature distribution for different time series can be determined using different parameters (relative humidity, wind speed and direction, atmospheric water content, etc.) and different algorithms. Landsat thermal bands being widely available have an effective potential to be used in drought monitoring, spatial-temporal climatic changes, early warning and protection of ecosystem with their temporal resolution capabilities in lake environments. And also representative climatic and hydrologic data provided vital information about the environmental and hydrological conditions. Therefore, these remote sensing techniques are important tools for the lake utilizers in terms of developing management strategies for natural resources.

In this regard, it is thought that the temperature data obtained by using the thermal bands of the satellites can be used in modeling studies for climate change by supporting them with long-term on-site measurement data. However, the surface temperature data derived for the study area can also be used to form the basis for drought monitoring, future climate studies and management plans for soil, land and water resources.

ACKNOWLEDGEMENTS

This research includes a part of the author Cansu Yurteri's PhD thesis. This research is supported by Hacettepe University Scientific Research Projects Coordination Unit (Project No: 18960-2021). The authors are thankful to the United States Geological Research Center (USGS) for providing the Landsat satellite images accessible, the General Directorate of Meteorology of the Ministry of Agriculture and Forestry for the meteorological data. And also this study was presented in International Online Conference on

Engineering and Natural Sciences (IOCENS'21), 5-7 July 2021.

AUTHORSHIP CONTRIBUTIONS

Authors equally contributed to this work.

DATA AVAILABILITY STATEMENT

The authors confirm that the data that supports the findings of this study are available within the article. Raw data that support the finding of this study are available from the corresponding author, upon reasonable request.

CONFLICT OF INTEREST

The author declared no potential conflicts of interest with respect to the research, authorship, and/or publication of this article.

ETHICS

There are no ethical issues with the publication of this manuscript.

REFERENCES

- [1] Lamaro A, Mariñelarena A, Torrusio S, Sala S. Water surface temperature estimation from Landsat 7 ETM+ thermal infrared data using the generalized single-channel method: Case study of Embalse del Río Tercero (Córdoba, Argentina). *Advances in Space Research* 2012;51. [\[CrossRef\]](#)
- [2] Sharaf N, Fadel A, Bresciani M, Giardino C, Lemaire B, Slim K, Faour G, Vinçon-Leite B. Lake surface temperature retrieval from Landsat-8 and retrospective analysis in Karaoun Reservoir, Lebanon. *J Appl Remote Sens* 2019;13. [\[CrossRef\]](#)
- [3] Yang K, Yu Z, Luo Y, Zhou X, Shang C. Spatial-Temporal Variation of Lake Surface Water Temperature and Its Driving Factors in Yunnan-Guizhou Plateau. *Water Resour Res* 2019;55:4688–4703. [\[CrossRef\]](#)
- [4] Malik MS, Shukla JP. Retrieving of land surface temperature using thermal Remote Sensing and GIS techniques in Kandaihimmat watershed, Hoshangabad, Madhya Pradesh. *J Geol Soc India* 2018;92:298–304. [\[CrossRef\]](#)
- [5] Taloor AK, Manhas DS, Girish CK. Retrieval of land surface temperature, normalized difference moisture index, normalized difference water index of the Ravi basin using Landsat data. *Appl Comput Geosci* 2021;9:100051. [\[CrossRef\]](#)
- [6] Şekertekin A, Bonafoni S. Land surface temperature retrieval from Landsat 5, 7, and 8 over rural areas: assessment of different retrieval algorithms and emissivity models and toolbox implementation. *Remote Sensors* 2020;12:294. [\[CrossRef\]](#)

- [7] Avdan U, Jovanovska G. Algorithm for automated mapping of land surface temperature using Landsat 8 satellite data. *J Sensors* 2016;1–8. [CrossRef]
- [8] Şener E. Determination of seasonal changes in Burdur lake surface water temperature using Landsat 8 satellite images. *J Eng Sci Design* 2016;4:67–73. [CrossRef]
- [9] Anderson MC, Allen RG, Morse A, Kustas WP. Use of Landsat thermal imagery in monitoring evapotranspiration and managing water resources. *Remote Sensing Environ* 2012;122:50–65. [CrossRef]
- [10] Sobrino JA, Li ZL, Stoll MP, Becker F. Multichannel and multi-angle algorithms for estimating sea and land surface temperature with ATSR data. *Int J Remote Sensing* 1996;17:2089–2114. [CrossRef]
- [11] Wang F, Qin Z, Song C, Tu L, Karnieli A, Zhao S. An improved mono-window algorithm for land surface temperature retrieval from Landsat 8 thermal infrared sensor data. *Remote Sensing* 2015;7:4268–4289. [CrossRef]
- [12] Yu X, Guo X, Wu Z. Land surface temperature retrieval from Landsat 8 TIRS-comparison between radiative transfer equation-based method, split window algorithm and single channel method. *Remote Sensing* 2014;6:9829–9852. [CrossRef]
- [13] Jimenez-Munoz JC, Sobrino JA. A generalized single-channel method for retrieving land surface temperature from remote sensing data. *J Geophys Res* 2003;108:4688–4694. [CrossRef]
- [14] Gillespie AR, Rokugawa S, Matsunaga T, Cothorn JS, Hook SJ, Kahle AB. A temperature and emissivity separation algorithm for advanced space borne thermal emission and reflection radiometer (Aster) images. *IEEE Trans Geosci Remote Sensing* 1998;36:1113–1126. [CrossRef]
- [15] Qin Z, Karnieli A, Berliner P. A mono-window algorithm for retrieving land surface temperature from Landsat TM data and its application to the Israel-Egypt border region. *Int J Remote Sensing* 2010;22:3719–3746. [CrossRef]
- [16] Artis DA, Carnahan WH. Survey of emissivity variability in thermography of urban areas. *Remote Sensing Environ* 1982;12:313–329. [CrossRef]
- [17] Reis S, Yilmaz H. Temporal monitoring of water level changes in Seyfe Lake using remote sensing. *Hydrol Proces* 2008;22:4448–4454. [CrossRef]
- [18] Yaman M, Yigit Avdan Z. Monitoring water body change with using satellite images (Seyfe Lake) VII. *Remote Sensing ve GIS Symposium (UZAL-CBS)*, September 2018; Eskişehir, Turkey.
- [19] Palmer SC, Kutser T, Hunter PD. Remote sensing of inland waters: Challenges, progress and future directions *Remote Sensing Environ* 2015;157:1–8. [CrossRef]
- [20] Xu H. Modification of normalised difference water index (NDWI) to enhance open water features in remotely sensed imagery. *Int J Remote Sensing* 2006;27:3025–3033. [CrossRef]
- [21] <https://earthexplorer.usgs.gov>. 11 October 2021.
- [22] Chander G, Markham BL, Helder DL. Summary of current radiometric calibration coefficients for Landsat MSS, TM, ETM+ and EO1 ALI sensors. *Remote Sensing Environ* 2009;113:893–903. [CrossRef]
- [23] USGS, Landsat 8 data users handbook, Ed. Zanter, K., EROS Sioux Falls, South Dakota, USA, 2019. p. 114.
- [24] Olioso A, Sarrío MM, Courault D, Marloie O, Guillevic P. Impact of surface emissivity and atmospheric conditions on surface temperatures estimated from top of canopy brightness temperatures derived from Landsat 7 data. *IEEE International Geoscience and Remote Sensing Symposium* 2013; Melbourne, Australia. [CrossRef]
- [25] Kriegler FJ, Malila WA, Nalepka RF, Richardson W. Preprocessing transformations and their effects on multispectral recognition. *Remote Sensing Environ* 1969;6:97.
- [26] Carlson TN, Ripley DA. On the relation between NDVI, fractional vegetation cover, and leaf area index. *Remote Sensing of Environment* 62,1997;62:241–252. [CrossRef]
- [27] Norman JM, Becker F. Terminology in thermal infrared remote sensing of natural surfaces. *Agric Forest Meteorol* 1995;77:153–166. [CrossRef]